Dynamic Plume Tracking by Cooperative Robots

Jun-Wei Wang, Yi Guo, Muhammad Fahad and Brian Bingham

Abstract—This paper presents cooperative control of autonomous mobile robots to monitor and track dynamic pollutant plume propagation in m-dimensional space. The dynamics of the pollutant plume is modeled by an advection-diffusion partial differential equation (PDE), and the plume front is described by a level set with a pre-specified threshold value. We solve the problem of cooperative plume tracking using two cooperating robots under formation control, one is assigned as the sensing robot and the other is assigned as the tracking robot, where the sensing robot estimates the gradient and divergence information of the entire field based on its current concentration measurement, and the tracking robot tracks the plume front and patrols on it. Rigorous convergence analysis is provided using the set stability concept. Numerical simulations of pollutant plume tracking in both 2-D and 3-D spaces demonstrate the effectiveness of the proposed control scheme. This paper extends existing literature from static level curve tracking to dynamic plume front tracking, and presents a PDE-observer based plume front tracking control design. The results are applicable to emerging environmental monitoring tasks by cooperative robots.

Index Terms—Cooperative control, Mobile robots, Dynamic pollutant plume, Set stability, Partial differential equation.

I. INTRODUCTION

ARINE pollution is one of the major environment hazards as it not only leads to serious economic losses in coastal areas but also causes long-term damage to the marine environment [1]. For oil spill response management, one needs to effectively track the oil plume boundary to determine the spatial extent of the spill. This mission poses great challenges due to the dynamic nature of plume propagation and the complexity of oceanographical processes. Thanks to recent advances in sensors, robotics, and control techniques in marine mechatronic systems [2]-[4], mobile robots equipped with chemical sensors have been used to monitor pollutant plumes in marine environments [5], [6], and networks of multiple robots are ideal candidates for large-scale persistent environmental monitoring (e.g., large forest fires, oil spill, floods [7]— [9], mine countermeasure [10], and aquatic environment [11]). We study cooperative plume tracking control in this paper. A motivating application scenario is shown in Fig. 1, where two unmanned surface vessels (USVs) cooperatively monitor the plume propagation while maintaining formation in the sea.

This work was partially supported by the National Science Foundation under Grants IIS-1218155 and CMMI-1527016.

Jun-Wei Wang is with the School of Automation and Electrical Engineering, University of Science and Technology Beijing, Beijing 100083, P. R. China. E-mail: junweiwang@ustb.edu.cn. This work was done when Jun-Wei Wang was a postdoctoral researcher at Stevens Institute of Technology.

Yi Guo and Muhammad Fahad are with Department of Electrical and Computer Engineering, Stevens Institute of Technology, Hoboken, NJ 07030, USA. E-mails: {yguo1,mfahad}@stevens.edu.

Brian Bingham is with Mechanical and Aerospace Engineering, Naval Postgraduate School, Monterey, CA 93943, USA. E-mail: bbingham@nps.edu.

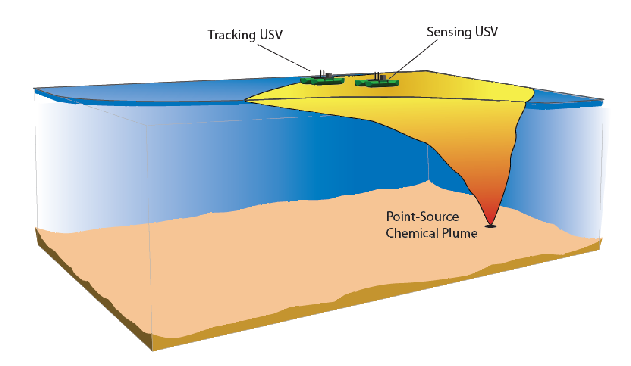


Fig. 1: Motivating example: Dynamic plume tracking by USVs. The USVs are assigned to the roles of sensing and tracking, and they cooperatively monitor the plume front propagation while maintaining formation.

A. Related Work

Tracking environmental boundaries by a robotic network has attracted much attention from both controls and robotics communities over the past decade. A comprehensive survey of algorithms for boundary estimation and tracking using collaborating sensors was provided in [12]. Existing methods on environmental boundary tracking can be classified as the gradient-free approach and the gradient-based approach. For the gradient-free approach, research results have been reported such as mapping-based tracking [13]- [16], bio-inspired tracking [17]- [19], bang-bang tracking control [20], [21], and adaptive tracking control [22]. Utilizing the gradient information of the plume from the environmental field, gradient-based tracking algorithms have been developed in [23]- [30] with rigorous mathematical analysis. The controllers in [23]- [26] were developed with direct access to the gradient, but how to obtain the gradient information was not addressed therein. To derive the gradient information, a least-squared estimation was proposed in [27]. In [28] and [29], the gradient information was obtained from a cooperative filter with the Hessian matrix derived by a separate cooperative filter via the Frenet-Serret equation and the least-squared method. It is worth noting that the aforementioned work deals with static fields only. However, the environmental fields (e.g. oil plume fields) are almost never static and often cannot be well approximated by static fields.

Control methods were reported in [31] for multi-agent autonomous vehicles to perform the exploration of *non-stationary* environments, motivated by the results in [23] and [24]. In [32], a library of reactive motion control algorithms was proposed (including a random coverage controller, a collision avoidance controller, and a bang-bang angular velocity controller) to detect and surround an dynamic perimeter. By combing the results [21] and [33], a sliding mode guidance and

control method was presented in [34] for tracking of moving and deforming environmental level sets of general dynamic fields. In [35], a cooperative control algorithm was provided that allows a mobile sensor network to track and distribute along a stable dynamic boundary of the environment, where the dynamic boundary is defined by ODEs and assumed stable in the sense that its parameter vector converges to a constant vector as time elapses. The aforementioned work does not take into consideration of specific spatiotemporal evolutional dynamics of the pollution field in the environment.

Motivated by the fact that the spatiotemporal dynamics of the pollution plume field can be modeled by distributed parameter systems (DPSs) described by partial differential equations (PDEs) [36]- [43], we propose a PDE-observer design to estimate a spatiotemporally evolving field for the purpose of tracking control. PDE-observer based estimation was recently studied in [44]-[47] for DPSs with a mobile sensor or sensor network. In our group's earlier conference paper [48], observer-based cooperative control algorithms were developed for multi-robots to monitor and track dynamic plume fronts, where the plume was modeled by a 2-D advection-diffusion PDE and the extended Luenberger observer was applied to estimate the plume front dynamics. Since the assumption made in [48] on the availability of the gradient and the divergence information may be too strong for real-world applications. we develop in this paper a Luenberger-type PDE observer to online estimate the gradient and divergence thus the strong assumption is removed.

B. Main Contribution

In this paper, we study cooperative plume front tracking of dynamic pollutant dispersion in an m-dimensional space (m-D space) by two autonomous robots, where the dynamics of a pollutant plume is described by an m-D advection-diffusion PDE, and the plume front is described by a level set with a pre-specified value. We propose a cooperative plume tracking scheme, where two robots are assigned the roles of sensing and tracking, respectively. A distributed-parameter Luenberger observer is developed on the sensing robot to estimate the concentration field over the entire spatial domain, and a motion control law is constructed on the tracking robot to drive the robot to the plume front utilizing the estimated concentration information from the sensing robot. Meanwhile, the sensing robot is regulated to form a desired formation with the tracking robot. Rigorous convergence analysis is provided using set stability concepts of DPSs. The developed algorithm is tested in simulations for pollutant plume tracking in both 2-D and 3-D spaces, which show satisfactory performances.

The contributions of the paper are twofold. First, we develop a distributed-parameter Luenberger observer to estimate the concentration field based on point-wise sensor measurements, which is used to obtain the gradient and divergence information consequently for plume front tracking control of robots. Second, we extend the dynamic plume estimation and tracking from the 2-D space to the m-D space.

Comparing to existing work, we consider *dynamic* pollutant plume tracking where the plume spreads along time, while

many other work (e.g., [28]–[30]) discusses *static* level curve tracking. Different from existing work on boundary tracking of *dynamic* environmental fields (e.g., [34]), where the dynamics of environmental fields is not taken into account, we utilize an advection-diffusion PDE model and estimate the spatiotemporal evolution of the concentration field. While the recent work [46] uses similar advection-diffusion PDE to model dynamic pollutant dispersion, it focuses on sensing and estimation without tracking, and the results are limited to the 2-D space. Comparing to our own conference publication [48], we remove the impractical assumption that both gradient and divergence information are available for tracking control, propose a new distributed-parameter Luenberger observer design, and extend the result to the general *m*-D space.

C. Organization and Notations

The rest of the paper is organized as follows. Section II introduces system models, definitions of set stability and problem formulation. Section III presents two-robot cooperative plume front tracking control design. Extensive numerical simulation results are provided in Section IV to show the effectiveness of the proposed control algorithm. Finally, Section V offers brief concluding remarks and future work.

 \mathfrak{R} and \mathfrak{R}^n denote the set of all real numbers and $n\text{-}\mathrm{D}$ Euclidean space with the norm $\|\cdot\|$, respectively. For a vector $\mathbf{a} \in \mathfrak{R}^n$, \mathbf{a}^{\perp} denotes an orthogonal vector of \mathbf{a} , i.e., $\mathbf{a}^T \mathbf{a}^{\perp} = 0$. $\mathcal{H}^n \triangleq \mathcal{L}_2(\Omega; \mathfrak{R}^n)$ is a separable Hilbert space of n-D vector functions that is equipped with the inner product $\langle \cdot, \cdot \rangle$ and induced norm $\|\cdot\|_2 \triangleq \sqrt{\langle\cdot,\cdot\rangle}$, where Ω is a bounded and convex spatial domain in \Re^m . $|\cdot|_2 \triangleq \sqrt{\langle \cdot, \cdot \rangle}$ is the norm of the separable Hilbert space $\mathcal{H} \triangleq \mathcal{L}_2(\Omega; \mathfrak{R})$ of scalar functions. $\mathcal{W}^{k,2}(\Omega;\mathfrak{R})$ is a Sobolev space of absolutely continuous scalar functions with square integrable derivatives of the order k > 1. $\nabla \cdot$ is the divergence of a continuously differentiable vector field $\boldsymbol{v}(\boldsymbol{x},t)$ with respect to \boldsymbol{x} , i.e., $\nabla \cdot \boldsymbol{v}(\boldsymbol{x},t) = \sum_{i=1}^{m} \frac{\partial v_i(\boldsymbol{x},t)}{\partial x_i}$. $diag\{a_1 \ a_2 \ \cdots \ a_n\}$ is a diagonal matrix with elements $a_i \in \mathfrak{R}, i \in \{1, 2, \cdots, n\}$. For a scalar variable $\theta \in \mathfrak{R}$ and any subinterval Ω_0 containing zero in \Re , $\delta(\theta)$ is a Dirac delta function [49] defined as $\delta(\theta) = \infty$ if $\theta = 0$, otherwise $\delta(\theta) = 0$, and $\int_{\Omega_0} \delta(\theta) d\theta = 1$. For a vector variable $\boldsymbol{\alpha} \triangleq [\alpha_1 \ \alpha_2 \ \cdots \ \alpha_n]^T \in \mathfrak{R}^n$, $\delta(\boldsymbol{\alpha}) = \delta(\alpha_1) \delta(\alpha_2) \cdots \delta(\alpha_n)$.

II. SYSTEM MODELS AND PROBLEM FORMULATION

In this section, we present the plume and the robot model, definitions for the set stability and set tracking, and formulate the control problem addressed in this paper.

A. Dynamic Plume Model of Pollutant Dispersion

The dynamic plume of pollutant dispersion is in general modeled by the following advection-diffusion PDE system in an m-D space with a state-space description of the following form [48]:

$$\frac{\partial C(\mathbf{x}, t)}{\partial t} + \mathbf{v}^{T}(\mathbf{x}, t) \nabla C(\mathbf{x}, t) = \nabla \cdot (\mathbf{D} \nabla C(\mathbf{x}, t))$$
$$t \ge t_0, \ \mathbf{x} \in \Omega$$
 (1)

subject to the Dirichlet boundary conditions

$$C(\mathbf{x},t)|_{\mathbf{x}\in\partial\Omega} = 0, \ t \ge t_0,$$
 (2)

and the initial condition

$$C(\mathbf{x}, t_0) = C_0(\mathbf{x}), \ \mathbf{x} \in \Omega, \tag{3}$$

where $0 \le C(\cdot, t) \in \mathcal{H}$ is the pollutant concentration at the time t and the position $\mathbf{x} \triangleq [x_1 \ x_2 \ \cdots \ x_m]^T \in \Omega \subset \mathfrak{R}^m$, Ω is the given region under consideration for pollutant dispersion, e.g., a rectangle in \Re^2 and a cube in \Re^3 ; $\frac{\partial C(\mathbf{x},t)}{\partial t}$ is the partial derivative of $C(\mathbf{x},t)$ with respective to the time t, $\boldsymbol{v}(\boldsymbol{x},t) \triangleq [v_1(\boldsymbol{x},t) \ v_2(\boldsymbol{x},t) \ \cdots \ v_m(\boldsymbol{x},t)]^T \in \mathfrak{R}^m$ is the velocity field of the medium (e.g., the water for underwater chemical pollutant or the air for gaseous pollution), where thermical point of the air of gaseous point only, $\nabla C(\boldsymbol{x},t) \triangleq \left[\frac{\partial C(\boldsymbol{x},t)}{\partial x_1} \ \frac{\partial C(\boldsymbol{x},t)}{\partial x_2} \ \cdots \ \frac{\partial C(\boldsymbol{x},t)}{\partial x_m}\right]^T \in \Re^m \text{ is the spatial gradient of } C(\boldsymbol{x},t), \boldsymbol{D} \triangleq \operatorname{diag}\{d_1 \ d_2 \ \cdots \ d_m\} > 0$ is the eddy diffusion coefficient matrix, $\nabla \cdot (\mathbf{D}\nabla C(\mathbf{x},t)) =$ $\sum_{i=1}^{m} d_i \frac{\partial^2 C(\mathbf{x},t)}{\partial x_i^2}$ is the divergence of $\mathbf{D} \nabla C(\mathbf{x},t)$, and $t_0 > 0$ is the time when the pollutant dispersion occurs. The term $\boldsymbol{v}^T(\boldsymbol{x},t)\nabla C(\boldsymbol{x},t)$ models the advection of the plume caused by the medium flow (e.g., the water flow or the air flow). The term $\nabla \cdot (\mathbf{D}\nabla C(\mathbf{x},t))$ describes the eddy diffusion of the pollutant plume in the medium, which describes the motion from higher concentration area to the lower concentration area. The term $\partial\Omega$ denotes the boundary of the spatial domain Ω , and $C_0(x)$, $x \in \Omega$, is the pollutant concentration value in the spatial domain Ω at the time t_0 . Note that the value of m for the pollutant plume in real-world settings is chosen from the set $\{2,3\}$, i.e., $m \in \{2,3\}$.

We make an assumption for the velocity field v(x, t).

Assumption 1: In the spatial domain Ω , the velocity field $\boldsymbol{v}(\boldsymbol{x},t)$ is known and its divergence $\nabla \cdot \boldsymbol{v}(\boldsymbol{x},t)$ is zero, i.e., $\nabla \cdot \boldsymbol{v}(\boldsymbol{x},t) = 0$ for all $t \geq t_0$ and $\boldsymbol{x} \in \Omega$.

The flow field $\boldsymbol{v}(\boldsymbol{x},t)$ in a given spatial domain Ω can be obtained from sensors or sustained observation data of the spatial domain. For example, robot mounted acoustic Doppler current profilers (ADCPS) provide accurate velocity profiles in real-time, or use NASA's ocean and climate datasets [50] available to get certain areas' current flow information. The constraint $\nabla \cdot \boldsymbol{v}(\boldsymbol{x},t) = 0$ is naturally fulfilled for an incompressible flow field $\boldsymbol{v}(\boldsymbol{x},t)$, as the pressure constrains the flow so that the volume of fluid elements is a constant, i.e., the isochoric flow resulting in a solenoidal velocity field with $\nabla \cdot \boldsymbol{v}(\boldsymbol{x},t) = 0$ [51]. This flow field $\boldsymbol{v}(\boldsymbol{x},t)$ is in general modeled by the incompressible Navier-Stokes equations [51] and [52]. In general, for most applications in the ocean and many in the atmosphere, one can assume that the fluid medium is approximately incompressible.

B. Mobile Robot Model

To facilitate the control algorithm development, we assume that the robot's kinematic model is described by a fully actuated single integrator equation

$$\dot{\boldsymbol{x}}_r = \boldsymbol{u}_r, \ t \ge t_d, \ \boldsymbol{x}_r(t_d) = \boldsymbol{x}_{r0}, \tag{4}$$

where $\mathbf{x}_r \in \mathfrak{R}^m$ and $\mathbf{u}_r \in \mathfrak{R}^m$ are the state and control input of the robot in an m-D workspace, respectively, and $t_d >$

0 ($t_d \ge t_0$) is the time when the robot is deployed to the pollutant plume field $C(\mathbf{x},t)$ at the position \mathbf{x}_{r0} of Ω . Note that the kinematic model of unmanned surface vehicles [53] can be transformed to the above single-integrator model [48].

C. Set Stability

Level sets have been commonly used to describe contours of a field (e.g., the concentration field, the temperature field, and the flow field) or environmental boundaries ([20], [21], [23]-[29], [34], [48]). For a dynamic concentration field $C(\mathbf{x},t)$, define the set

$$\mathbb{L}_{\mathbb{S}}(C, C_L) \triangleq \{ \boldsymbol{x}_L \in \mathfrak{R}^m \mid C(\boldsymbol{x}_L, t) = C_L \}, \tag{5}$$

where C_L is the constant value of the level of interest. Clearly, due to the space distribution of the field $C(\mathbf{x},t)$, this set is an infinite-dimensional set for $m \geq 2$, i.e., this set contains an infinite number of elements \mathbf{x}_L . Moreover, the set $\mathbb{L}_{\mathbb{S}}(C,C_L)$ is bounded and closed. Since the Hilbert space \mathcal{H} is separable, it can be easily verified that the level set $\mathbb{L}_{\mathbb{S}}(C,C_L)$ is compact (Lemma 1 of [54]).

In what follows, we introduce rigorous mathematical definitions of set stability and set tracking. The "distance" between the robot and the contour described by the set $\mathbb{L}_{\mathbb{S}}(C,C_L)$ is defined as

$$\|\mathbf{x}_r\|_{\mathbb{L}_{\mathcal{S}}(C,C_L)} \triangleq |C(\mathbf{x}_r,t) - C_L|. \tag{6}$$

where $C(\mathbf{x}_r, t)$ is the concentration value at the robot's position \mathbf{x}_r and time t.

The following two definitions are given that will be used later for convergence analysis.

Definition 1: The robot is **set** stable with respect to $\mathbb{L}_{\mathbb{S}}(C,C_L)$ if for any time t_d and any scalar $\varepsilon>0$, there exists a scalar $\nu(\varepsilon,t_d)>0$ such that

$$\|\mathbf{x}_{r0}\|_{\mathbb{L}_{\mathbb{S}}(C,C_L)} < \nu(\varepsilon,t_d) \Rightarrow \|\mathbf{x}_r\|_{\mathbb{L}_{\mathbb{S}}(C,C_L)} < \varepsilon, \quad \forall \ t \ge t_d.$$
 (7)

Moreover, if ν in (7) is independent of t_d , the robot is said to be *uniformly set stable* with respect to $\mathbb{L}_{\mathbb{S}}(C, C_L)$.

Definition 2: The set tracking with respect to $\mathbb{L}_{\mathbb{S}}(C, C_L)$ for the robot is achieved if

$$\lim_{t \to +\infty} \|\mathbf{x}_r\|_{\mathbb{L}_{\mathcal{S}}(C, C_L)} = 0 \tag{8}$$

for any initial conditions x_{r0} and $C(x_{r0}, t_d)$.

Remark 1: The concept of set stability has previously been introduced in [55] to discuss the coordination problem of multi-agent systems, including the target aggregation to a convex set and the state agreement. The definition of set tracking has also been defined to address the problem of connectivity and set tracking of multi-agent systems with multiple moving leaders [56]. Different from the definitions of set stability [55] and set tracking [56], which are defined for a finite-dimensional set (i.e., a set contains a finite number of elements), Definitions 1 and 2 here are provided for an infinite-dimensional set which involves an infinite number of elements.

D. Problem Formulation

Based on the above models and definitions, we present our control problem of cooperative plume tracking addressed in this paper. Here we consider the problem of two-robot cooperative plume front tracking. For these two robots, we assign one as the *tracking robot* that is equipped an onboard sensor to measure the concentration value for tracking and patrolling the plume front, and the other as the *sensing robot* that has an onboard sensor to measure the concentration value and can estimate the gradient and the divergence information of the field. We assume bi-directional communication between the two robots, that is, the robots can both send and receive information from each other.

Let us define $x_r \in \mathfrak{R}^m$, $u_r \in \mathfrak{R}^m$, $x_s \in \mathfrak{R}^m$, and $u_s \in \mathfrak{R}^m$ as the state and control input for the tracking robot and the sensing robot, respectively. The tracking robot has the kinematic model (4), and the sensing robot is modeled by the following fully actuated single integrator equation

$$\dot{\boldsymbol{x}}_s = \boldsymbol{u}_s, \ t \ge t_d, \ \boldsymbol{x}_s(t_d) = \boldsymbol{x}_{s0}, \tag{9}$$

where $t_d > 0$ $(t_d \ge t_0)$ is the time when the sensing robot is deployed to the pollutant plume field $C(\mathbf{x},t)$ at the position \mathbf{x}_{s0} of Ω .

We assume both the sensing and the tracking robots have point-wise sensor concentration measurements. The concentration measurements are denoted as

$$y_s(\mathbf{x}_s, t) = \int_{\Omega} \delta(\mathbf{x} - \mathbf{x}_s) C(\mathbf{x}, t) d\mathbf{x} = C(\mathbf{x}_s, t), \quad (10)$$

$$y_r(\mathbf{x}_r, t) = \int_{\Omega} \delta(\mathbf{x} - \mathbf{x}_r) C(\mathbf{x}, t) d\mathbf{x} = C(\mathbf{x}_r, t), \qquad (11)$$

where $y_s(\mathbf{x}_s, t)$ is the sensing robot measurement, and $y_r(\mathbf{x}_r, t)$ is the tracking robot measurement.

Let the set $\mathbb{L}_{\mathbb{S}}(C,C_f) \triangleq \{x_f \in \mathfrak{R}^m | C(x_f,t) = C_f\}$ be the plume front, where $C_f > 0$ is the threshold concentration. The control task is to drive the tracking robot to reach the plume front $\mathbb{L}_{\mathbb{S}}(C,C_f)$ and patrol on this plume front, based on the concentration measurements $y_s(x_s,t)$ and $y_r(x_r,t)$ defined above. Meanwhile, the two robots maintain a desired formation. This control task is formally stated as follows.

Cooperative Plume Tracking Problem: For the dynamic pollutant plume modeled by (1)-(3) satisfying Assumption 1, we will develop a cooperative control algorithm for two cooperating robots with the concentration measurements $y_s(\mathbf{x}_s,t)$ in (10) and $y_r(\mathbf{x}_r,t)$ in (11), such that the *tracking robot* reaches the plume front $\mathbb{L}_{\mathbb{S}}(C,C_f)$ as the time elapses, and patrols on this plume front with a desired speed v_{dc} . Meanwhile, two cooperating robots maintain a desired formation.

III. COOPERATIVE PLUME TRACKING CONTROL DESIGN

This section focuses on the development of the observerbased control framework for cooperative plume front tracking. The following Luenberger-type PDE observer for the estimation of dynamic concentration field $C(\mathbf{x},t)$ is constructed by using the concentration measurement $y_s(\mathbf{x}_s,t)$ as

$$\frac{\partial \hat{C}(\mathbf{x},t)}{\partial t} + \mathbf{v}^{T}(\mathbf{x},t)\nabla \hat{C}(\mathbf{x},t) = \nabla \cdot (\mathbf{D}\nabla \hat{C}(\mathbf{x},t))
+ L\delta(\mathbf{x} - \mathbf{x}_{s})(y_{s}(\mathbf{x}_{s},t) - \hat{y}_{s}(\mathbf{x}_{s},t)),
\hat{C}(\mathbf{x},t)\Big|_{\mathbf{x}\in\partial\Omega} = 0, \ \hat{C}(\mathbf{x},t_{d}) = \hat{C}_{t_{d}}(\mathbf{x}) \neq 0,
\hat{y}_{s}(\mathbf{x}_{s},t) = \int_{\Omega} \delta(\mathbf{x} - \mathbf{x}_{s})\hat{C}(\mathbf{x},t)d\mathbf{x} = \hat{C}(\mathbf{x}_{s},t), \quad (12)$$

where $\hat{C}(\mathbf{x},t)$ is the estimated concentration field over the spatial domain Ω , L>0 is a constant observer gain, and $\hat{C}_{t_d}(\mathbf{x})$ is the estimated concentration field information in the spatial domain Ω when the sensing robot is initially deployed to the field.

Let $\tilde{C}(\mathbf{x},t) \triangleq C(\mathbf{x},t) - \hat{C}(\mathbf{x},t)$ be the observer error. It is then governed by the following error system:

$$\frac{\partial \tilde{C}(\mathbf{x},t)}{\partial t} + \mathbf{v}^{T}(\mathbf{x},t)\nabla \tilde{C}(\mathbf{x},t) = \nabla \cdot (\mathbf{D}\nabla \tilde{C}(\mathbf{x},t))
- L\delta(\mathbf{x} - \mathbf{x}_{s})\tilde{C}(\mathbf{x}_{s},t),$$

$$\tilde{C}(\mathbf{x},t)\Big|_{\mathbf{x}\in\partial\Omega} = 0, \ \tilde{C}(\mathbf{x},t_{d}) = \tilde{C}_{t_{d}}(\mathbf{x}),$$
(13)

where $\tilde{C}_{t_d}(\mathbf{x}) \triangleq C(\mathbf{x}, t_d) - \hat{C}_{t_d}(\mathbf{x})$.

Note that as the observer (12) on the sensing robot estimates the concentration value of the whole field, the gradient and divergence information at the tracking robot's position can be obtained, which will be used next for the control design of the tracking robot.

Based on the dynamic equation of the Luenberger observer (12), we propose the following control law for the tracking robot:

$$\boldsymbol{u}_r = \frac{\hat{f}(\boldsymbol{x}_r)\nabla\hat{C}(\boldsymbol{x}_r,t)}{\|\nabla\hat{C}(\boldsymbol{x}_r,t)\|^2} + \frac{\upsilon_{dc}\nabla^{\perp}\hat{C}(\boldsymbol{x}_r,t)}{\|\nabla^{\perp}\hat{C}(\boldsymbol{x}_r,t)\|},$$
(14)

where v_{dc} is the desired patrolling speed of the tracking robot along the plume front, and

$$\hat{f}(\mathbf{x}_r) \triangleq -k_1 e_{y_r}(\mathbf{x}_r, t) - \nabla \cdot (\mathbf{D} \nabla \hat{C}(\mathbf{x}_r, t)) + \mathbf{v}^T(\mathbf{x}_r, t) \nabla \hat{C}(\mathbf{x}_r, t),$$
(15)

in which $e_{y_r}(\mathbf{x}_r, t)$ is the error of the concentration measurement $y_r(\mathbf{x}_r, t)$ at the robot's position \mathbf{x}_r and the one at the plume front $\mathbb{L}_{\mathbb{S}}(C, C_f)$, that is,

$$e_{y_r}(\mathbf{x}_r, t) \triangleq y_r(\mathbf{x}_r, t) - C_f. \tag{16}$$

It is seen that the control law (14) consists of two parts: $\frac{\hat{f}(\mathbf{x}_r)\nabla\hat{C}(\mathbf{x}_r,t)}{\|\nabla\hat{C}(\mathbf{x}_r,t)\|^2} \text{ and } \frac{v_{dc}\nabla^\perp\hat{C}(\mathbf{x}_r,t)}{\|\nabla^\perp\hat{C}(\mathbf{x}_r,t)\|}.$ The first one ensures the tracking robot achieving the basic control objective — reaching the plume front $\mathbb{L}_{\mathbf{S}}(C,C_f)$, and the second one guarantees the tracking robot achieving the second control objective — patrolling on the plume front with a desired speed v_{dc} . Obviously, the control law (14) requires $\|\nabla\hat{C}(\mathbf{x}_r,t)\| \neq 0$ and $\|\nabla^\perp\hat{C}(\mathbf{x}_r,t)\| \neq 0$, $t>t_d$. To do this, the initial value $\hat{C}_{t_d}(\mathbf{x})$ in the observer (12) is chosen such that $\nabla\hat{C}_{t_d}(\mathbf{x}) \neq 0$.

Next, we will construct a control law for the sensing robot by using formation control techniques and the control law (14). Define e_d be a formation error of the tracking robot and the sensing one, i.e.,

$$\boldsymbol{e}_d \triangleq \boldsymbol{x}_s - \boldsymbol{x}_r + \boldsymbol{\sigma}_d, \tag{17}$$

where $\sigma_d \neq 0$ is a desired formation specification.

Using formation control techniques, the control law (14), and (17), the control law for the sensing robot is given as

$$\boldsymbol{u}_s = \boldsymbol{u}_r - k_2 \boldsymbol{e}_d - \dot{\boldsymbol{\sigma}}_d \tag{18}$$

where $k_2 > 0$ is a given constant and \boldsymbol{u}_r is the control law given in (14). Note that the desired formation, $\boldsymbol{\sigma}_d$, is chosen based on the application. As the tracking robot patrols on the plume front, we may choose $\boldsymbol{\sigma}_d \triangleq -d \frac{\nabla \hat{C}(\boldsymbol{x}_r,t)}{\|\nabla \hat{C}(\boldsymbol{x}_r,t)\|}$ to describe a desired side-by-side formation with the sensing robot placed inside of the plume, where d>0 is the Euclidean distance between the sensing robot and the tracking robot.

Remark 2: As defined in the subsection II-D, we assume bi-directional communication between the tracking and sensing robots. Specifically, the tracking robot sends its current position \mathbf{x}_r and control input \mathbf{u}_r to the sensing robot for cooperative formation, and the sensing robot sends the tracking robot information including the estimates of the gradient and divergence at the tracking robot's current position (i.e., $\nabla \hat{C}(\mathbf{x}_r, t)$ and $\nabla \cdot (\mathbf{D} \nabla \hat{C}(\mathbf{x}_r, t))$) based on the observer result running onboard of the sensing robot.

The following theorem states our main result on the cooperative tracking control scheme.

Theorem 1: Consider the dynamic pollutant plume described by (1)-(3) with Assumption 1, and the two cooperating robots, the tracking robot and the sensing robot, are driven by the control laws (14) and (18), respectively. For any given constant control gains $k_1>0,\ k_2>0$, and the observer gain L>0, we can obtain:

- a). The observer error system (13) is exponentially stable in the sense of $|\cdot|_2$, i.e., $|\tilde{C}(\cdot,t)|_2 \to 0$ as $t \to \infty$.
- b). The control law (18) drives the sensing robot to maintain a desired formation σ_d with the tracking robot, i.e., $\|\boldsymbol{e}_d\|^2 \to 0$ as $t \to \infty$.
- c). The control law (14) drives the tracking robot to achieve the *set tracking* with respect to the set $\mathbb{L}_{\mathbb{S}}(C,C_f)$ and patrol on the plume front $\mathbb{L}_{\mathbb{S}}(C,C_f)$ with a desired speed v_{dc} in the sense of $\frac{(\nabla^{\perp}\hat{C}(\mathbf{x}_r,t))^T}{\|\nabla^{\perp}\hat{C}(\mathbf{x}_r,t)\|}$ $\dot{\mathbf{x}}_r = v_{dc}$.

That is, the tracking robot and sensing robot driven by the control laws (14) and (18) with observer (12), respectively, solve the **Cooperative Plume Tracking Problem**.

Proof: See the Appendix.

Remark 3: Note that the Dirac delta function $\delta(\cdot)$ is used in our observer (12). This function was similarly used in [46] to solve concentration estimation of a moving gaseous source in a 2-D space using a sensing aerial vehicle, and in [57] to address adaptive output feedback control of a 2-D linear diffusion PDE system with spatially collocated mobile actuator/sensor pairs. It was pointed out in [49] that the explicit form of $\delta(\cdot)$ can be given by

$$\delta(x) = \left\{ \begin{array}{ll} 0 & \text{otherwise} \\ \lim_{\varepsilon \to 0} \varepsilon^{-1} & \text{if } x \in (-0.5\varepsilon, 0.5\varepsilon). \end{array} \right.$$

For numerical implementation, one can use the following approximation [45], [49]

$$\delta(x) \approx \delta_{\varepsilon}(x) \tag{19}$$

where ε is a small positive constant given in advance and

$$\delta_{\varepsilon}(x) \triangleq \left\{ \begin{array}{ll} 0 & \text{otherwise} \\ \varepsilon^{-1} & \text{if } x \in (-0.5\varepsilon, 0.5\varepsilon). \end{array} \right.$$

Remark 4: In our group's early work [48], a model-based control algorithm was developed for the problem of single robot dynamic plume tracking under the strong assumption that both the gradient and the divergence information at the robot position are available. In this paper, we remove the strong assumption on the availability of the gradient and divergence, construct a Luenberger-type PDE observer from the concentration measurement of the sensing robot to estimate the concentration of the dynamic field, and propose an observer-based tracking control design (i.e., Theorem 1) for the tracking robot to track the dynamic plume front.

Remark 5: In our proposed cooperative plume tracking algorithm, the motion of the sensing robot is guided by the formation control, which achieves a pre-designated desired formation with the tracking robot. Hence, the motion control of the sensing robot is independent of the observer design, and a distributed parameter observer is constructed without considering the motion of the sensing robot. When implementing the algorithm, we may choose the desired formation to facilitate sensing. For example, as the tracking robot patrols on the plume front, we may choose a desired side-by-side formation with the sensing robot placed inside of the plume. However, it should be noted that the formation control does not guarantee best sensing performances in general, as the estimation performance of the observer is indeed affected by the guidance control law of the sensing robot due to the dependence of the concentration measurement $y_s(x_s, t)$ on the sensing robot's position x_s . The problem of integrated design of observers and motion guidance for state estimation of DPSs is out of the scope of the current paper.

IV. NUMERICAL SIMULATIONS

In this section, we present numerical simulation results on dynamic plume tracking for point-wise source chemical pollutant introduced into the water, and the effectiveness of the proposed cooperative tracking control scheme is demonstrated. Cooperative tracking in both 2-D and 3-D cases are shown.

A. Environment Simulation

We simulate both 2-D and 3-D ocean environments for chemical plume dispersion. The simulation of the environment includes the simulator of a flow field v(x,t) and the simulator of the concentration field C(x,t).

Flow Field Generation: In 2-D space, the flow field is generated numerically by solving the incompressible Navier-Stokes equation in the domain Ω with prescribed velocities along the boundary using the program reported in [52]. The flow field in 2-D space is visualized in Fig. 2, where the strength and direction of the flow at various positions are

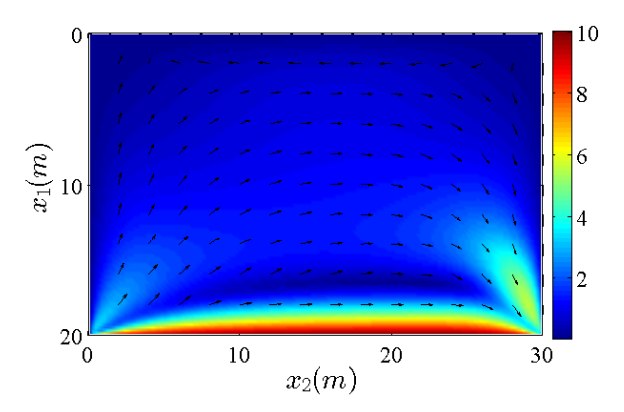


Fig. 2: The flow velocity field v(x,t) considered in this simulation, where the pseudo-color and the black arrow indicate the strength and the direction of the flow velocity, respectively.

shown. In 3-D space, for simplicity, the flow velocity field $\boldsymbol{v}(\boldsymbol{x},t)$ in the spatial domain Ω is set to be time-invariant and space-invariant, *i.e.*, $\boldsymbol{v}(\boldsymbol{x},t) = \boldsymbol{v}_0$ where \boldsymbol{v}_0 is a constant vector, which is chosen as $\boldsymbol{v}(\boldsymbol{x},t) = [2\ 2\ 2]^T$ in our simulation.

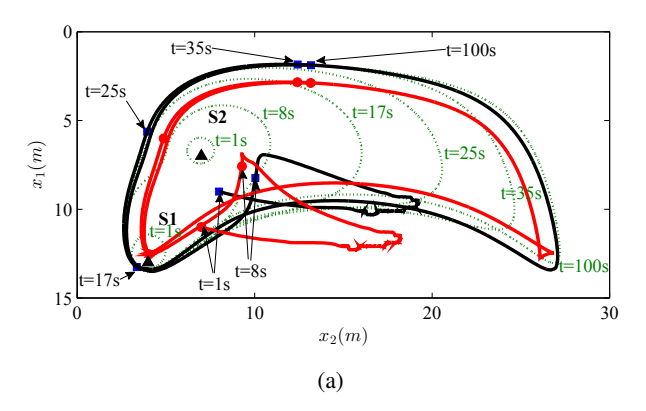
Concentration Field Generation: Two chemical sources with different constant concentration values are set at different locations of the domain Ω . The propagation of the chemical in the flow field results in a *dynamic* concentration field, which is generated by solving the advection-diffusion PDE system (1)-(3) with the zero initial condition (*i.e.*, $C_0(\mathbf{x}) = 0$) and the appropriate diffusion coefficient \mathbf{D} .

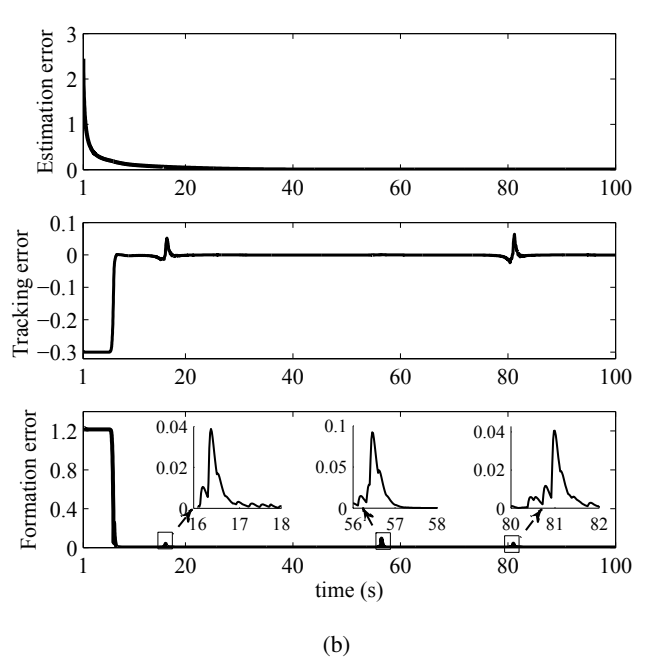
In 2-D space, a rectangular spatial domain Ω is set to be $\Omega \triangleq [0\ 20] \times [0\ 30]$. Two chemical sources, denoted as S1 and S2, are set at the locations $[13\ 4]^T$ and $[7\ 7]^T$, where the concentration values of S1 and S2 are 3 and 2, respectively. The concentration value of the plume front is set as $C_f = 0.3$. The diffusion coefficient \mathbf{D} is set as $\mathbf{D} = \mathrm{diag}\{0.5\ 0.5\}$ [48]. In 3-D space, a cubic spatial domain Ω is set to be $\Omega \triangleq [0\ 12] \times [0\ 12] \times [0\ 12]$. Two chemical sources, denoted as S1 and S2, are set at the positions $[3\ 2\ 1]^T$ and $[1\ 2\ 1]^T$ with the fixed concentration values 8 and 7, respectively. The concentration value of the plume front is set as $C_f = 0.1$. The diffusion coefficient \mathbf{D} is set as $\mathbf{D} = \mathrm{diag}\{0.5\ 0.5\ 0.1\}$.

B. Cooperative Plume Tracking

We present in this subsection simulations of the cooperative plume front tracking, and verify Theorem 1 for both 2-D and 3-D cases.

In 2-D Space: Here we verify the cooperative plume front tracking algorithm for the two cooperating USVs, i.e., Theorem 1 for 2-D space case. In the simulation, set $\nabla^{\perp}\hat{C}(\mathbf{x}_r,t) = \begin{bmatrix} 0 & 1 \\ -1 & 0 \end{bmatrix} \nabla\hat{C}(\mathbf{x}_r,t), \ \boldsymbol{\sigma}_d = -\frac{\nabla\hat{C}(\mathbf{x}_r,t)}{\|\nabla\hat{C}(\mathbf{x}_r,t)\|}, \ v_{dc} = 1, \ k_1 = 10, \ k_2 = 10 \ \text{and} \ L = 30.$ The initial value for the Luenberger-type PDE observer of the form (12) is set to be $\hat{C}_{t_d}(\mathbf{x}) = 20(x_1/20)^3(1-x_1/20)^3(x_2/30)^3(1-x_2/30)^3, \ \text{which satisfies} \ \nabla\hat{C}_{t_d}(\mathbf{x}) \neq 0.$ At $t_d = 1s, i.e.$, one second after the sources start propagation at time $t_0 = 0s$, the tracking robot and the sensing robot are deployed to the field at the positions $[8\ 9]^T$ and $[7\ 11]^T$.





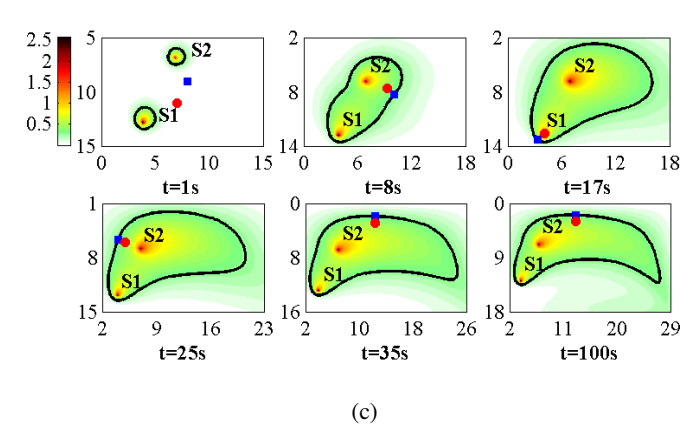


Fig. 3: Cooperative plume front tracking in 2-D space. (a) Trajectories of the robots and the plume propagation. Green curves: plume front contour; Black curves: tracking robot's trajectory; Red curve: sensing robot's trajectory; Blue squares: tracking robot's positions at various times; Red circles: sensing robot's positions at various times. (b) The trajectories of observer error, $|\tilde{C}(\cdot,t)|_2^2$, tracking error, $e_{y_r}(x_r,t)$, and formation error, $\|\boldsymbol{e}_d\|$. (c) Snapshots of the robot movements.

Fig. 3 shows the simulation results. As shown in Fig. 3 (a), the robots' trajectories (marked as red and black solid curves) move towards the plume front (marked as green dotted curves) as time elapses, and meantime, the sensing robot (in red) and the tracking robot (in black) form a side-by-side formation with the sensing robot placed inside the plume. Specifically, when the robots are initially deployed, the observer error is big, so the robots move away from the plume. As the observer error gets smaller along the time, both of the sensing and tracking robots move on the plume front after t = 8s. As shown in Fig. 3 (b), the plume front tracking error, $e_{y_r}(\mathbf{x}_r, t)$, reduces to zero as time elapses. We define the formation error, $\|e_d\|$, to be the Euclidean distance between the two robots. It can be seen in Fig. 3 (b), the formation error approaches to its desired formation, σ_d , i.e., $\|\mathbf{e}_d\| \to 0$ as $t \to \infty$. Note that two peaks appear at around t = 16.6s and t = 81.2sin the tracking error, and three small peaks appear at around t = 16.3s, t = 56.5s and t = 81s in the formation error in Fig. 3 (b) when the robots travel across the lower left and right tip of the plume front curve where the geometric shape of the plume front curve changes sharply, and the concentration at the lower left tip changes sharply. Fig. 3 (c) shows the snapshots of the robots' motion and the plume propagation at various times.

In 3-D Space: Now we show the performance of our cooperative plume front tracking given in Theorem 1 in 3-

D space. Set
$$\nabla^{\perp} \hat{C}(\mathbf{x}_r,t) = \begin{bmatrix} 0 & -1 & -1 \\ 1 & 0 & -1 \\ 1 & 1 & 0 \end{bmatrix} \nabla \hat{C}(\mathbf{x}_r,t),$$
 $v_{dc} = 3, \ k_1 = 10, \ \boldsymbol{\sigma}_d = \begin{bmatrix} 2 & 0 & 0 \end{bmatrix}^T, \ k_2 = 4, \ \text{and} \ L = 10.$ The initial value for the Luenberger-type PDE observer (12) is set to be $\hat{C}_{t_d}(\mathbf{x}) = 1000(x_1/12)^3(1-x_1/12)^3(x_2/12)^3(1-x_2/12)^3(x_3/12)^3(1-x_3/12)^3$, which satisfies $\nabla \hat{C}_{t_d}(\mathbf{x}) \neq 0$.

Here the robots are deployed to the positions $[4 \ 4 \ 6]^T$ and $[3 \ 3 \ 6]^T$ at time $t_d = 1$ s, while the chemical sources start propagation at time $t_0 = 0s$. Fig. 4 (a) presents the simulation results, where the trajectories of the tracking and the sensing robots are shown together with the plume front propagation. We can see from Fig. 4 (a) that as time elapses, the sensing robot (in red) and the tracking robot (in black) converge to the plume front (marked as the pink contour) and form a side-byside formation. Similar to the simulation results in Fig. 3 for 2-D space, when the robots are initially deployed, the observer error makes the robots move away from the plume, see Fig. 4 (a). As time elapses, the observer error reduces to zero and the robots move on the plume front after t = 5s. The tracking error and the formation error are shown in Fig. 4 (b). It can be seen that as the time elapses, the control law (14) drives the tracking robot to reach the plume front and patrol on it. Meanwhile, the control law (18) guides the sensing robot form a desired formation with the tracking robot.

C. Robustness Discussion

Notice that the model-based cooperative control scheme in Theorem 1 is developed under the assumption that the plume propagation model is known and the robots can obtain the concentration measurements timely and accurately. However, in practices, there are uncertainties in the plume model, and the concentration measurements may not be accurate due to the existence of sensor noises. Furthermore, the communication between the sensing and the tracking robots may not be perfect, and packet loss may exist due to communication constraints.

We demonstrate the simulation results of the proposed cooperative control scheme in the presence of plume model uncertainties, imperfect measurements, and packet loss in communications, and discuss the robustness of the suggested cooperative control scheme. To this end, we set the plume model (1) be subject to the model uncertainties, i.e., adding the perturbation 0.01D in the coefficient matrix D, and adding the external disturbance $0.3\cos(\pi t)\exp(-0.1t)$ in model (1). The concentration measurements $y_r(\mathbf{x}_r, t)$ and $y_s(\mathbf{x}_s, t)$ in (10) and (11) are added pseudo-random noises drawn from the standard uniform distribution on the open intervals (0,0.07)and (0,0.05). We also add the packet loss that is modeled by a Bernoulli distribution [58] with the probability of success rate 0.95. Fig. 5 shows the trajectory of the observer error, $|C(\cdot,t)|_2^2$, the tracking error, $e_{y_r}(\mathbf{x}_r,t)$, and the formation error, $\|\mathbf{e}_d\|$, in 2-D space and 3-D space, where we can see that the tracking and formation errors converge but are less smooth and have more oscillations comparing to performances shown in Figs. 3 (b) and 4 (b) due to the effect of uncertainties. It can be seen that the proposed cooperative tracking control algorithm is applicable to plume tracking in the presence of the aforementioned uncertainties, although the performance is degraded comparing to the cases without uncertainties.

V. CONCLUSIONS AND FUTURE WORK

We presented robot plume front tracking of dynamic pollutant dispersion in the *m*-D space in this paper by two cooperating robots. An observer-based control algorithm was proposed to solve the cooperative plume tracking. The suggested control strategy guarantees the tracking robot reaching the plume front, patrolling on it, and forming a desired formation with the sensing robot. To obtain the gradient and divergence information through point-wise sensor concentration measurement only, a distributed-parameter Luenberger observer was designed to estimate the concentration field over the entire spatial domain. Rigorous convergence analysis was given in light of set stability concepts of DPSs. Extensive numerical simulations are shown for pollutant plume tracking in both 2-D and 3-D spaces, which demonstrated the effectiveness of the proposed cooperative control scheme.

The paper presents an estimation and control framework for environmental monitoring tasks applicable to ocean plume front tracking by USVs. The proposed scheme can be extended both theoretically and practically. In the future work, we are interested in extending the proposed observer-based control to the case of multiple robot plume front tracking and patrolling, where communication graphs are defined among N robots, and boundary and follower robot controllers are constructed separately. Our previous work [48] shows some preliminary results with this idea. We are also interested in extending the proposed observer-based tracking control design to the source

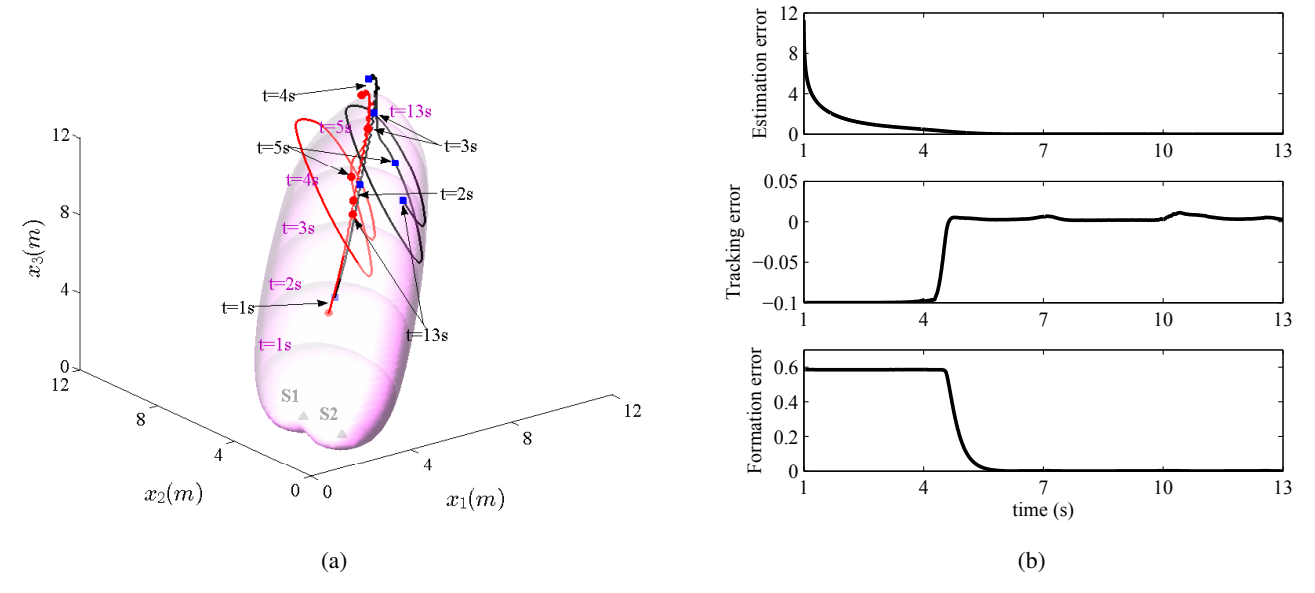


Fig. 4: Cooperative plume front tracking in 3-D space. (a) Trajectories of the tracking and the sensing robots. Pink contours: plume propagation; Black curves: tracking robot's trajectory; Red curves: sensing robot's trajectory; Blue squares: tracking robot's positions at various times; Red circles: sensing robot's positions at various times. (b) The trajectories of observer error, $|\tilde{C}(\cdot,t)|_2^2$, tracking error, $e_{y_r}(\mathbf{x}_r,t)$, and formation error, $\|\mathbf{e}_d\|$.

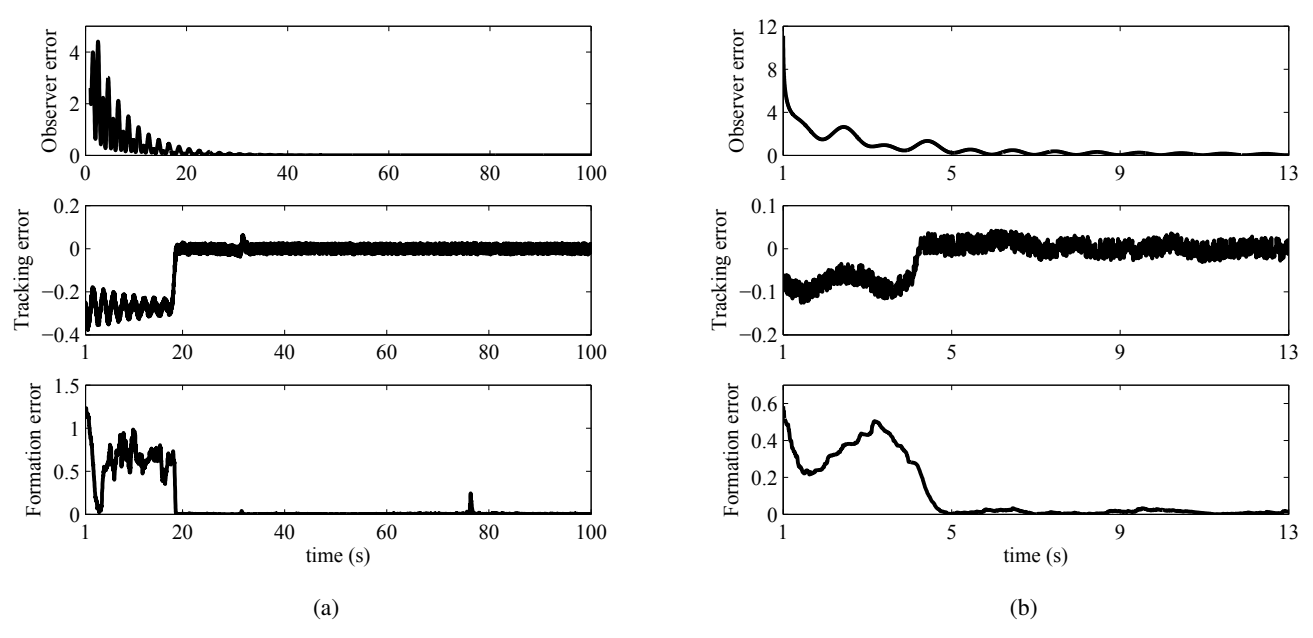


Fig. 5: Cooperative plume front tracking in the presence of plume model uncertainties, imperfect concentration measurements, and packet loss: The trajectories of observer error, $|\tilde{C}(\cdot,t)|_2^2$, tracking error, $e_{y_r}(\mathbf{x}_r,t)$, and formation error, $\|\mathbf{e}_d\|$, in: (a) 2-D space, and (b) 3-D space.

seeking problem ([59]) to identify the location of the plume source. Furthermore, extending the 3D tracking control to heterogenous robot platforms with authentic vehicle dynamics, such as USVs and unmanned underwater vehicles (UUVs), is important from a practical point of view. Other interesting future work includes optimal guidance control for the sensing robot and integrated design of observers and motion guidance for state estimation of DPSs as mentioned in Remark 5 of the paper.

APPENDIX PROOF OF THEOREM 1

Proof: In the proof, using Lyapunov's stability based methods, we construct Lyapunov functions to analyze stabilities of: 1) the observer error system, 2) the formation error system, and 3) the tracking error system.

1). Stability analysis of observer error system (13): Consider the following Lyapunov functional candidate for exponential stability analysis of the observer error system (13):

$$V_1(t) = 0.5 \int_{\Omega} \tilde{C}^2(\mathbf{x}, t) d\mathbf{x}. \tag{20}$$

The time derivative of the Lyapunov functional $V_1(t)$ along the solution to the observer error system (13) is presented as

$$\dot{V}_{1}(t) = \int_{\Omega} \tilde{C}(\mathbf{x}, t) \nabla \cdot (\mathbf{D} \nabla \tilde{C}(\mathbf{x}, t)) d\mathbf{x}
- \int_{\Omega} \tilde{C}(\mathbf{x}, t) \boldsymbol{v}^{T}(\mathbf{x}, t) \nabla \tilde{C}(\mathbf{x}, t) d\mathbf{x}
- L \int_{\Omega} \delta(\mathbf{x} - \mathbf{x}_{s}) \tilde{C}(\mathbf{x}, t) d\mathbf{x} \tilde{C}(\mathbf{x}_{s}, t)
= - \int_{\Omega} \nabla^{T} \tilde{C}(\mathbf{x}, t) \mathbf{D} \nabla \tilde{C}(\mathbf{x}, t) d\mathbf{x}
- 0.5 \int_{\Omega} \nabla \cdot \boldsymbol{v}(\mathbf{x}, t) \tilde{C}^{2}(\mathbf{x}, t) d\mathbf{x} - L \tilde{C}^{2}(\mathbf{x}_{s}, t).$$
(21)

Note that the second equal sign holds because of the following equations and the *sifting property* for the Dirac delta function $\delta(x)$ [49]:

$$\int_{\Omega} \tilde{C}(\mathbf{x}, t) \nabla \cdot (\mathbf{D} \nabla \tilde{C}(\mathbf{x}, t)) d\mathbf{x} = -\int_{\Omega} \nabla^{T} \tilde{C}(\mathbf{x}, t) \mathbf{D} \nabla \tilde{C}(\mathbf{x}, t) d\mathbf{x},$$

and

$$\int_{\Omega} \tilde{C}(\mathbf{x},t) \boldsymbol{\upsilon}^T(\mathbf{x},t) \nabla \tilde{C}(\mathbf{x},t) d\mathbf{x} = -\frac{1}{2} \int_{\Omega} \nabla \cdot \boldsymbol{\upsilon}(\mathbf{x},t) \tilde{C}^2(\mathbf{x},t) d\mathbf{x},$$

which are derived by using Green formula and taking into account of the boundary conditions of (13).

Based on Assumption 1, we obtain

$$\int_{\Omega} \nabla \cdot \boldsymbol{v}(\boldsymbol{x}, t) \tilde{C}^{2}(\boldsymbol{x}, t) d\boldsymbol{x} = 0.$$
 (22)

Employing the Poincaré inequality [60] and considering $D = \text{diag}\{d_1, d_2, \dots, d_m\} > 0$, we have

$$\int_{\Omega} \nabla^{T} \tilde{C}(\mathbf{x}, t) \mathbf{D} \nabla \tilde{C}(\mathbf{x}, t) d\mathbf{x} \ge \mu \min_{1 \le i \le m} \{d_{i}\} \int_{\Omega} \tilde{C}^{2}(\mathbf{x}, t) d\mathbf{x}$$
(23)

where $\mu > 0$ is the Poincaré constant. Substitution of (22) and (23) into (21) and consider L > 0 and (20), we can give

$$\dot{V}_1(t) \le -2\mu \min_{1 \le i \le m} \{d_i\} V_1(t). \tag{24}$$

One derives from (24) that $|\tilde{C}(\cdot,t)|_2^2 \leq |\tilde{C}_{t_d}(\cdot)|_2^2 \exp(-2\mu \min_{1\leq i\leq m}\{d_i\}(t-t_d)),\ t>t_d$. That is,

$$|\tilde{C}(\cdot,t)|_2^2 \to 0 \text{ as } t \to \infty,$$
 (25)

i.e., the observer error system (13) is exponentially stable.

2). Formation performance analysis of the control law (18) for the sensing robot:

From (4), (9), and (18), the formation error e_d defined by (17) is governed by

$$\dot{\boldsymbol{e}}_d = -k_2 \boldsymbol{e}_d. \tag{26}$$

For the purpose of exponential stability analysis of the system (26), consider the following Lyapunov function candidate:

$$V_2(t) = 0.5 \boldsymbol{e}_d^T \boldsymbol{e}_d. \tag{27}$$

The time derivative of $V_2(t)$ given in (27) along the solution to the system (26) can be given as

$$\dot{V}_2(t) = \boldsymbol{e}_d^T \dot{\boldsymbol{e}}_d = -k_2 \boldsymbol{e}_d^T \boldsymbol{e}_d = -2k_2 V_2(t). \tag{28}$$

From (28), we obtain

$$\|\mathbf{e}_d\| = \|\mathbf{e}_{d0}\| \exp(-k_2(t - t_d)), \ t > t_d,$$
 (29)

where $\mathbf{e}_{d0} \triangleq \mathbf{x}_{s0} - \mathbf{x}_{r0} + \mathbf{\sigma}_{d0}$ with $\mathbf{\sigma}_{d0} \triangleq -d\frac{\nabla \hat{C}(\mathbf{x}_{r0},t_d)}{\|\nabla \hat{C}(\mathbf{x}_{r0},t_d)\|}$, i.e., $\|\mathbf{e}_d\| \to 0$ as $t \to \infty$. That is, the controller (18) drives the sensing robot to maintain the desired formation $\mathbf{\sigma}_d$ with respect to the tracking one. We can also obtain from (29) that $\mathbf{x}_r - \mathbf{x}_s \neq 0$ if $\mathbf{x}_{r0} \neq \mathbf{x}_{s0}$. According to the definition of $\delta(\cdot)$, we get if $\mathbf{x}_{r0} \neq \mathbf{x}_{s0}$,

$$\delta(\mathbf{x}_r - \mathbf{x}_s) = 0. ag{30}$$

3). Tracking performance analysis of the control law (14) for the tracking robot:

Substituting (14) into (4), we obtain the following closed-loop system for the tracking robot:

$$\dot{\boldsymbol{x}}_r = \frac{\hat{f}(\boldsymbol{x}_r)\nabla\hat{C}(\boldsymbol{x}_r,t)}{\|\nabla\hat{C}(\boldsymbol{x}_r,t)\|^2} + \frac{\upsilon_{dc}\nabla^{\perp}\hat{C}(\boldsymbol{x}_r,t)}{\|\nabla^{\perp}\hat{C}(\boldsymbol{x}_r,t)\|}.$$
 (31)

Using the following two facts:

$$\nabla^T \hat{C}(\mathbf{x}_r,t) \frac{\hat{f}(\mathbf{x}_r) \nabla \hat{C}(\mathbf{x}_r,t)}{\|\nabla \hat{C}(\mathbf{x}_r,t)\|^2} = \hat{f}(\mathbf{x}_r)$$

and

$$\nabla^T \hat{C}(\mathbf{x}_r,t) \frac{\upsilon_{dc} \nabla^{\perp} \hat{C}(\mathbf{x}_r,t)}{\|\nabla^{\perp} \hat{C}(\mathbf{x}_r,t)\|} = 0,$$

and considering (31), we can get

$$\nabla^T \hat{C}(\mathbf{x}_r, t) \dot{\mathbf{x}}_r = \hat{f}(\mathbf{x}_r). \tag{32}$$

To analyze the tracking performance of the control law (14) for the tracking robot, define $\hat{e}_C(\mathbf{x}_r,t)$ be the error of the estimated concentration value $\hat{C}(\mathbf{x}_r,t)$ at the robot's position \mathbf{x}_r and the one at the plume front $\mathbb{L}_{\mathbb{S}}(C,C_f)$, that is,

$$\hat{e}_C(\mathbf{x}_r, t) \triangleq \hat{C}(\mathbf{x}_r, t) - C_f. \tag{33}$$

Since $C_f > 0$ is a constant, applying the chain derivation rule and using (30), (32), and the observer system (12), the estimated tracking error $\hat{e}_C(\mathbf{x}_r, t)$ is governed by

$$\frac{d\hat{e}_C(\mathbf{x}_r, t)}{dt} = -k_1 \hat{e}_C(\mathbf{x}_r, t) + k_1 \tilde{C}(\mathbf{x}_r, t), \tag{34}$$

where $C(\mathbf{x}_r, t)$ is the value of the observer error $C(\mathbf{x}, t)$ at the robot's position \mathbf{x}_r .

We construct the following Lyapunov function candidate for the estimated tracking error system (34):

$$V_3(t) = 0.5\hat{e}_C^2(\mathbf{x}_r, t). \tag{35}$$

The time derivative of $V_3(t)$ given in (35) along the solutions to the system (34) is given as

$$\dot{V}_3(t) = -k_1 \hat{e}_C^2(\mathbf{x}_r, t) + k_1 \hat{e}_C(\mathbf{x}_r, t) \tilde{C}(\mathbf{x}_r, t). \tag{36}$$

Using the triangle inequality and considering $k_1 > 0$, the expression (36) is written as

$$\dot{V}_3(t) \le -0.5k_1 \hat{e}_C^2(\mathbf{x}_r, t) + 0.5k_1 \tilde{C}^2(\mathbf{x}_r, t)
= -k_1 V_3(t) + 0.5k_1 \tilde{C}^2(\mathbf{x}_r, t).$$
(37)

One can get from (37) that

$$\hat{e}_C^2(\mathbf{x}_r, t) \le \hat{e}_C^2(\mathbf{x}_{r0}, t_d) \exp(-k_1(t - t_d)) + 0.5k_1 \int_{t_d}^t \exp(-k_1(t - t_d - s)) \tilde{C}^2(\mathbf{x}_r, s) ds.$$
(38)

From (25), we obtain

$$\tilde{C}^2(\mathbf{x}_r, t) \to 0 \text{ as } t \to \infty.$$
 (39)

It can be derived from (38) and (39) that

$$\hat{e}_C^2(\mathbf{x}_r, t) \to 0 \text{ as } t \to \infty.$$
 (40)

On the other hand, by the definition of $e_{y_r}(\mathbf{x}_r, t)$ in (16), and (11), one can derive

$$|e_{y_r}(\mathbf{x}_r, t)|^2 = (y_r(\mathbf{x}_r, t) - C_f)^2 = (C(\mathbf{x}_r, t) - C_f)^2$$

$$= |\hat{e}_C(\mathbf{x}_r, t) + \tilde{C}(\mathbf{x}_r, t)|^2$$

$$\leq 2|\hat{e}_C(\mathbf{x}_r, t)|^2 + 2|\tilde{C}(\mathbf{x}_r, t)|^2.$$
(41)

Using (6), (39), (40), and considering (41), we know $\|\mathbf{x}_r\|_{\mathbb{L}_{\mathbb{S}}(C,C_f)}^2 = |e_{y_r}(\mathbf{x}_r,t)|^2 \to 0$ as $t \to \infty$ (i.e., $C(\mathbf{x}_r,t) \to C_f$ as $t \to \infty$). By Definition 2, the set tracking of the tracking robot with respect to the set $\mathbb{L}_{\mathbb{S}}(C,C_f)$ is ensured by the control law (14).

In a similar way, by using two facts $\frac{(\nabla^{\perp}\hat{C}(\mathbf{x}_r,t))^T}{\|\nabla^{\perp}\hat{C}(\mathbf{x}_r,t)\|} \frac{\hat{f}(\mathbf{x}_r)\nabla\hat{C}(\mathbf{x}_r,t)}{\|\nabla\hat{C}(\mathbf{x}_r,t)\|^2} = 0, \text{ and } \frac{(\nabla^{\perp}\hat{C}(\mathbf{x}_r,t))^T}{\|\nabla^{\perp}\hat{C}(\mathbf{x}_r,t)\|^2} \frac{v_{dc}\nabla^{\perp}\hat{C}(\mathbf{x}_r,t)\|^2}{\|\nabla^{\perp}\hat{C}(\mathbf{x}_r,t)\|} = v_{dc}, \text{ and considering (31),}$ we can get $\frac{(\nabla^{\perp}\hat{C}(\mathbf{x}_r,t))^T}{\|\nabla^{\perp}\hat{C}(\mathbf{x}_r,t)\|}\dot{\mathbf{x}}_r = v_{dc} \text{ for any } t \geq t_d, \text{ which implies that the tracking robot driven by the control law (14)}$ achieves the second control objective: the robot patrols on the plume front modeled by the set $\mathbb{L}_{\mathbf{S}}(C,C_f)$ with a given desired speed v_{dc} . This completes the proof.

REFERENCES

- B. Roach and J. M. Harris, *The Gulf Oil Spill: Economic and Policy Issues*. Medford: Global Development and Environmental Institute, 2010.
- [2] Z. Peng, D. Wang and J. Wang, Cooperative dynamic positioning of multiple marine offshore vessels: A modular design, *IEEE/ASME Trans. Mechatronics*, vol. 21, no. 3, pp. 1210–1221, 2016.
- [3] Z. Peng, J. Wang and D. Wang, Containment maneuvering of marine surface vehicles with multiple parameterized paths via spatial-temporal decoupling, *IEEE/ASME Trans. Mechatronics*, vol. 22, no. 2, pp. 1026– 1036, 2017.
- [4] Y. Shi, C. Shen, H. Fang, and H. Li, Advanced control in marine mechatronic systems: A survey, *IEEE/ASME Trans. Mechatronics*, vol. 22, no. 3, pp. 1121–1131, 2017.
- [5] R. Camilli, B. Bingham, M. Jakuba, H. Singh, and J. Whelan, Integrating in-situ chemical sampling with AUV control systems, in *Proc. 2004 MTS/IEEE Oceans Conf.*, vol. 1, pp. 101-109, 2004.
- [6] R. Camilli, B. Bingham, C. M. Reddy, R. K. Nelson, and A. N. Duryea, Method for rapid localization of seafloor petroleum contamination using concurrent mass spectrometry and acoustic positioning, *Marine Poll. Bull.*, vol. 58, no. 10, pp. 1505–1513, 2009.

- [7] A. Vasilijevic, D. Nad, F. Mandic, N. Miskovic, and Z. Vukic, Coordinated navigation of surface and underwater marine robotic vehicles for ocean sampling and environmental monitoring, *IEEE/ASME Trans. Mechatronics*, vol. 22, no. 3, pp. 1174–1184, 2017.
- [8] H. Ishida, Y. Wada, and H. Matsukura, Chemical sensing in robotic applications: A review, *IEEE Sensors J.*, vol. 12, no. 11, pp. 3163-3173, 2012.
- [9] M. Dunbabin and L. Marques, Robots for environmental monitoring: significant advancements and applications, *IEEE Trans. Robot. Autom. Mag.*, vol. 19, no. 1, pp. 24-39, 2012.
- [10] L. Paull, S. Saeedi, M. Seto, and H. Li, Sensor-driven online coverage planning for autonomous underwater vehicles, *IEEE/ASME Trans. Mechatronics*, vol. 18, no. 6, pp. 1827–1838, 2013.
- [11] J. Laut, E. Henry, O. Nov, and M. Porfiri, Development of a mechatronics-based citized science platform for aquatic environmental monitoring, *IEEE/ASME Trans. Mechatronics*, vol. 19, no. 5, pp. 1541– 1551, 2014.
- [12] S. Srinivasan, S. Dattagupta, P. Kulkarni, and K. Ramamritham, A survey of sensory data boundary estimation, covering and tracking techniques using collaborating sensors, *Pervasive Mob. Comput.*, vol. 8, no. 3, pp. 358-375, 2012.
- [13] J. A. Farrell, S. Pang, and W. Li, Plume mapping via hidden Markov methods, *IEEE Trans. Syst.*, *Man, Cybern. B, Cybern.*, vol. 33, no. 6, pp. 850-863, 2003.
- [14] A. Lilienthal and T. Duckett, Building gas concentration gridmaps with a mobile robot, *Robot. Auton. Syst.*, vol. 48, no. 1, pp. 3-16, 2004.
- [15] S. Pang and J. A. Farrell, Chemical plume source localization, *IEEE Trans. Syst., Man, Cybern. B, Cybern.*, vol. 36, no. 5, pp. 1068-1080, 2006.
- [16] G. Ferri, M. V. Jakuba, A. Mondini, V. Mattoli, B. Mazzolai, D. R. Yoerger, and P. Dario, Mapping multiple gas/odor sources in an uncontrolled indoor environment using a Bayesian occupancy grid mapping based method, *Robot. Auton. Syst.*, vol. 59, no. 11, pp. 988-1000, 2011.
- [17] W. Li, J. A. Farrell, S. Pang, and R. M. Arrieta, Moth-inspired chemical plume tracing on an autonomous underwater vehicle, *IEEE Trans. Robot.*, vol. 22, no. 2, pp. 292-307, 2006.
- [18] D. R. Webster, K. Y. Volyanskyy, and M. J. Weissburg, Bioinspired algorithm for autonomous sensor-driven guidance in turbulent chemical plumes, *Bioinspir. Biomim.*, vol. 7, no. 3, pp. 036023, 2012.
- [19] X. Kang and W. Li, Moth-inspired plume tracing via multiple autonomous vehicles under formation control, *Adapt. Behav.*, vol. 20, no. 2, pp. 131-142, 2012.
- [20] Z. Jin and A. L. Bertozzi, Environmental boundary tracking and estimation using multiple autonomous vehicles, in *Proc. 46th IEEE Conf. Decis. Control*, New Orleans, LA, pp. 4918-4923, 2007.
- [21] A. S. Matveev, H. Teimoori, and A. V. Savkin, Method for tracking of environmental level sets by a unicycle-like vehicle, *Automatica*, vol. 48, no. 9, pp. 2252-2261, 2012.
- [22] M. Malisoff and F. Zhang, Adaptive control for planar curve tracking under controller uncertainty, *Automatica*, vol. 49, no. 5, pp. 1411-1418, 2013.
- [23] D. Marthaler and A. Bertozzi, Collective motion algorithms for determining environmental boundaries, in *Proc. SIAM Conf. Appl. Dynamical Syst.*, Snowbird, UT, 2003.
- [24] D. Marthaler and A. L. Bertozzi, Tracking environmental level sets with autonomous vehicles, in *Recent Developments in Cooperative Control and Optimization*, S. Butenko, R. Murphey, and P. Pardalos Eds. Norwell, MA: Kluwer Academic Publishers, vol. 3, pp. 317-322, 2004.
- [25] A. L. Bertozzi, M. Kemp, and D. Marthaler, Determining environmental boundaries: Asynchronous communication and physical scales, in *Coop*erative Control, A Post-workshop Volume: 2003 Block Island Workshop on Cooperative Control, V. Kumar, N. Leonard,, A.S. Morse (eds). Springer, Germany, pp. 25-42, 2005.
- [26] T. Sun, H. Pei, Y. Pan, and C. Zhang, Robust adaptive neural network control for environmental boundary tracking by mobile robots, *Int. J. Robust Nonlin.*, vol. 23, no. 2, pp. 123-136, 2013.
- [27] P. Ogren, E. Fiorelli, and N. E. Leonard, Cooperative control of mobile sensor networks: Adaptive gradient climbing in a distributed environment, *IEEE Trans. Autom. Control*, vol. 49, no. 8, pp. 1292-1302, 2004.
- [28] F. Zhang and N. E. Leonard, Cooperative filters and control for cooperative exploration, *IEEE Trans. Autom. Control*, vol. 55, no. 3, pp. 650-663, 2010.
- [29] W. Wu and F. Zhang, Cooperative exploration of level surfaces of three dimensional scalar fields, *Automatica*, vol. 47, no. 9, pp. 2044-2051, 2011.

- [30] M. Malisoff and F. Zhang, Robustness of adaptive control under time delays for three-dimensional curve tracking, SIAM J. Control Optimi., vol. 53, no. 4, pp. 2203-2236, 2015.
- [31] I. Triandaf and I. B. Schwartz, A collective motion algorithm for tracking time-dependent boundaries, *Math. Comput. Simulat.*, vol. 70, no. 4, pp. 187-202, 2005.
- [32] J. Clark and R. Fierro, Mobile robotic sensors for perimeter detection and tracking, *ISA T.*, vol. 46, no. 1, pp. 3-13, 2007.
- [33] A. S. Matveev, H. Teimoori, and A. V. Savkin, Range-only measurements based target following for wheeled mobile robots, *Automatica*, vol. 47, no. 1, pp. 177-184, 2011.
- [34] A. S. Matveev, M. C. Hoy, A. M. Anisimov, and A. V. Savkin, Tracking of deforming environmental level sets of dynamic fields by a nonholonomic robot without gradient estimation, in *IEEE Int. Conf. Control Autom.*, Hangzhou, China, pp. 1754-1759, 2013.
- [35] Y. Cao and R. Fierro, Dynamic boundary tracking using dynamic sensor nets, in *Proc. 45th IEEE Conf. Decis. Control*, San Diego, CA, pp. 703-708, 2006
- [36] F. A. Zahor, W. M. Charles, and S. Mirau, Analysis and simulation of 3-D advection diffusion reaction model for pollutant dispersion, *J. Sci. Res. Stud.*, vol. 1, no. 2, pp. 9-16, 2014.
- [37] G. I. Marchuk, Mathematical Models in Environmental Problems, North Holland: Elsevier Science Publishers B.V., 1986.
- [38] P. Tkalich, MD. K. Huda, and K. Gin, A multiphase oil spill model, *J. Hydraul. Res.*, vol. 41, no. 2, pp. 115-125, 2003.
- [39] D. Kahforoshan, E. Fatehifar, A. A. Babalou, et al, Modeling and evaluation of air pollution from a gaseous flare in an oil and gas processing area, in WSEAS Conf. Spain, Spain, pp. 180-186, 2008.
- [40] J. M. Stockie, The mathematics of atmospheric dispersion modelling, SIAM Rev., vol. 53, no. 2, pp. 349-372, 2011.
- [41] A. Azevedo, A. Oliveira, A. B. Fortunato, and X. Bertin, Application of an Eulerian-Lagrangian oil spill modeling system to the prestige accident: trajectory analysis, *J. Coastal Res.*, Special Issue 56, pp. 777-781, 2009.
- [42] J. Wang and Y. Shen, Modeling oil spills transportation in seas based on unstructured grid, finite-volume, wave-ocean model, *Ocean Model.*, vol. 35, no. 4, pp. 332-344, 2010.
- [43] A. Ali, Modelling the dispersion of atmospheric pollutants dispersion using two dimensional advection diffusion equation, M. Sc. Dissertation, University of Dar es Salaam, 2011.
- [44] M. Demetriou and I. Hussein, Estimation of spatially distributed processes using mobile spatially distributed sensor network, SIAM J. Control Optimi., vol. 48, no. 1, pp. 266-291, 2009.
- [45] M. Demetriou, Guidance of mobile actuator-plus-sensor networks for improved control and estimation of distributed parameter systems, *IEEE Trans. Autom. Control*, vol. 55, no. 7, pp. 1570-1584, 2010.
- [46] M. Demetriou, N. Gatsonis, and J. Court, Coupled controls-computational fluids approach for the estimation of the concentration from a moving gaseous source in a 2-D domain with a Lyapunov-guided sensing aerial vehicle, *IEEE Trans. Control Syst. Technol.*, vol. 22, no. 3, pp. 853-867, 2014.
- [47] J.-W. Wang and Y. Guo, Distributed-parameter Luenberger observer for semi-linear parabolic PDE systems with a mobile pointwise sensor, in 35th Chinese Control Conf., Chengdu, China, pp. 1366–1371, 2016.
- [48] S. Li, Y. Guo, and B. Bingham, Multi-robot cooperative control for monitoring and tracking dynamic plumes, in *IEEE Int. Conf. Robot. Autom.*, Hongkong, China, pp. 67-73, 2014.
- [49] V. Balakrishnan, All about the Dirac delta function(?), Resonance, vol. 8, no. 8, pp. 48-88, 2003.
- [50] Dataset Discovery, Physical Oceanography Distributed Active Archive Center, http://podaac.jpl.nasa.gov/ datasetlist, NASA Jet Propulsion Laboratory, Accessed Oct. 2015.
- [51] G. K. Batchelor, An Introduction to Fluid Dynamics, New York: Cambridge University Press, 1967.
- [52] B. Seibold, A compact and fast MATLAB code solving the incompressible Navier-Stokes equations on rectangular domains, MIT, 2008.
- [53] C. R. Sonnenburg and C. A. Woolsey, Modeling, identification, and control of an unmanned surface vehicle, *J. Field Robot.*, vol. 30, no. 3, pp. 371-398, 2013.
- [54] R. A. Raimi, Compact transformations and the k-topology in Hilbert space, *Proc. Am. Math. Soc.*, vol. 6, no. 4, pp. 643-646, 1955.
- [55] G. D. Shi and Y. G. Hong, Global target aggregation and state agreement of nonlinear multi-agent systems with switching topologies, *Automatica*, vol. 45, no. 5, pp. 1165-1175, 2009.
- [56] G. D. Shi, Y. G. Hong and K. H. Johansson, Connectivity and set tracking of multi-agent systems guided by multiple moving leaders, *IEEE Trans. Autom. Control*, vol. 57, no. 3, pp. 663-676, 2012.

- [57] M. A. Demetriou, Adaptive control of 2-D PDEs using mobile collocated actuator/sensor pairs with augmented vehicle dynamics, *IEEE Trans. Autom. Control*, vol. 57, no. 12, pp. 2979–2993, 2012.
- [58] A. Klenke, *Probability Theory*, London: Springer-Verlag, 2006.
- [59] S. Li, R. Kong, and Y. Guo, Cooperative distributed source seeking by multiple robots: Algorithms and experiments, *IEEE/ASME Trans. Mechatronics*, vol. 19, no. 6, pp. 1810–1820, 2014.
- [60] G. Hardy, J. Littlewood, and G. Polya, *Inequalities*, 2nd ED. Cambridge: Cambridge University Press, 1952.



Jun-Wei Wang received the B.S. degree in mathematics and applied mathematics and the M.S. degree in system theory both from Harbin Engineering University, Harbin, China, in 2007 and 2009, and the Ph.D. degree in control theory and control engineering from Beihang University, Beijing, China, in 2013, respectively.

From March to September in 2012, he was a Research Assistant with the Department of Systems Engineering and Engineering Management, City University of Hong Kong. From September

2013 to December 2015, he was a Postdoctoral Researcher with the School of Automation and Electrical Engineering, University of Science and Technology Beijing. From August 2014 to July 2015, he was a Postdoctoral Researcher in the Department of Electrical and Computer Engineering, Stevens Institute of Technology, Hoboken, NJ, USA. In January 2016, he joined the School of Automation and Electrical Engineering, University of Science and Technology Beijing, where he is currently an Associate Professor.

His research interests include robust control and filtering, distributed parameter systems, and fuzzy/neural network modeling and control.



Yi Guo received the B.S. and M.S. from Xi'an University of Technology, Xi'an, China, in 1992 and 1995, respectively, and Ph.D. from the University of Sydney, Australia, in 1999, all in electrical engineering. She was a Postdoctoral Research Fellow at Oak Ridge National Laboratory from 2000 to 2002, and a Visiting Assistant Professor at the University of Central Florida, Orlando, FL, USA, from 2002 to 2005. She joined the Department of Electrical and Computer Engineering, Stevens Institute of Technology, Hoboken, NJ, USA, in 2005, where she is

currently a Professor.

Her main research interests include autonomous mobile robotics, distributed sensor networks, and nonlinear control systems. She has published more than 100 peer-reviewed journal and conference papers, authored the book entitled "Distributed Cooperative Control: Emerging Applications" (John Wiley & Sons 2017), and edited a book on micro/nano-robotics for biomedical applications (Springer 2013).



Muhammad Fahad received the B.S. in electrical engineering from University of Engineering and Technology, Lahore, Pakistan, in 2007, and M.S. in electrical engineering from Stevens Institute of Technology, Hoboken, NJ, in 2013. He is currently pursuing a Ph.D.degree in the Robotics and Automation Laboratory at Stevens Institute of Technology, Hoboken, NJ. His research interests include cooperative distributed localization, environmental monitoring, human robot interaction and reinforcement learning.



Brian Bingham received the B.S. degree (1996) from the Missouri University of Science and Technology, Rolla, MO, USA, and M.S. (1998) and PhD (2003) degrees from the Massachusetts Institute of Technology, Cambridge, MA, USA, all in mechanical engineering. He is currently an Associate Professor with the Department of Mechanical and Aerospace Engineering, Naval Postgraduate School, Monterey, CA, USA. His research interests include the design, dynamics and control of robotic systems.